 CMC, vol.12, no.1, pp.1-37, 2009

Bond-Slip Effects on the Behaviour of RC Beam under Monotonic Loading – An Integrated 3D Computational Model using EAS Approach

Amiya K. Samanta[1] **and Somnath Ghosh**[2]

Abstract: This paper presents a formulation of hypo-elasticity based RC beam model with bond-slip. Details of the constitutive model and analysis method used are provided. A procedure has been described to carry out three-dimensional analysis considering both geometrical as well as material nonlinearity for a simply supported RC beam employing finite element technique, which uses 8-noded isoparametric hexahedral element HCiS18. Enhanced assumed strain (EAS) formulation has been utilized to predict load-deformation and internal stresses both in the elastic as well as nonlinear regime. It models the composite behaviour of concrete and reinforcements in rigid /perfect bond situation and their mutual interaction in bond-slip condition considering continuous interface elements at the material level. An attempt has been made to reduce the gap significantly between the results found experimentally and numerically using the proposed model and a computer code has been developed for the purpose. The results of the analysis are presented, discussed and compared with a few benchmark experimental results.

Keywords: Lower order elements, Finite element approach, Three-dimensional, Enhanced assumed strain (EAS), Perfect bond, Bond-slip, RC beam.

1 Introduction

1.1 The problem

There are a variety of civil engineering structures with interface discontinuities, where the assumption of rigid bond between the mating surfaces is not valid. The analysis of such domain is accompanied by sliding, separation etc., which may occur along the interfaces between the adjacent blocks. In general, this phenomenon takes place at lower level of shear than the limiting shear value. As a result, an analysis procedure of such domain, which assumes rigid bond at the interface, would

[1] Civil Engineering Department, NIT, Durgapur, India. aksnitd@gmail.com
[2] Civil Engineering Department, Jadavpur University, Kolkata, India

over-predict the shear transfer and depending on the nature of the problem at hand, this would lead to either under-estimation or over-estimation of the response of the structure. Thus interconnection between the mating surfaces plays a major role in predicting overall response of a structure throughout its loading history. So an appropriate model is necessary to take into account of the relative movement of the two mating surfaces, in particular to the Reinforced Concrete (RC) structures.

RC structures are highly non-homogeneous medium due to discrete presence of the reinforcements. Till now only a few literatures have been reported, where investigator has prepared computational model of RC structures with concrete and the reinforcing steel having different physical and mechanical properties, which needs to be combined together through an interaction model to represent its composite behavior. Hence when RC structures are modeled based on continuum mechanics, contribution and distribution of stiffness of reinforcements should be given due importance along with the appropriate modeling of material parameters of parent domain, i.e. concrete. In fact, most of the commercial FE programs contain models, which are either too simple or too complex for design calculations. Hence there is a need for integrated system for nonlinear analysis with refinement at different levels. A major emphasis on modeling /establishing a proper interconnection has been given in this presentation in addition to different mechanical and physical properties of the parent material i.e. concrete and reinforcement.

1.2 Literature survey

The finite element technique, as a very important tool, has received a considerable interest of various authors for the purpose of analysis of discontinuous systems in particular the RC structures. The earliest work on such an application was done by Ngo and Scordelis (1967), where simple beam models were developed with constant strain triangles and a special bond link was used to describe the bond-slip effect. It was a case of linear analysis with predefined cracks to evaluate principal stresses both in concrete and reinforcement along with bond stresses. Nilson (1972) introduced nonlinear material properties for concrete and steel as well as nonlinear bond-slip relationship into the analysis to perform nonlinear analysis with the help of incremental load method. Attention was also given to introduce new crack direction in subsequent iterations. In line with the above, plane stress elements were also used by numerous investigators such as Nayak and Zienkiewicz (1972) etc., among others, for the same with an emphasis on constitutive relationships of the materials, cracking and elasto-plastic behavior, the effect of temperature, creep and shrinkage, tension stiffening. The concept of smeared crack approach introduced by Kollegger and Mehlhorn (1990) was preferred by the investigators to model the cracking phenomena in nonlinear analysis of RC structures, as its implementation

in finite element analysis is very straight forward than that of the discrete crack model. In this context, two different methods emerged viz. the fixed crack and the rotating crack model. In fixed crack model, cracks are supposed to form in a direction perpendicular to the principal stress direction when it exceeds concrete tensile strength and the crack direction remains unchanged in course of subsequent loading. In fact, it was well accepted by the researcher at the very early stages due to its easy formulation. Subsequent studies, however, showed that it causes numerical instability as a result of singularity in stiffness matrix and later on this difficulty was overcome by introducing variable cracked shear modulus by Balakrishnon and Murray (1988). In rotating crack model, crack direction changes with subsequent loading path depending on the current principal strain direction. Also the assumption of no shear strain in the crack plane eliminates the requirement of cracked shear modulus. This model is particularly useful in analytical studies of global behaviour of RC structures rather than the local effects in the vicinity of a crack. Ferretti et al. (2008) has recently also thrown some light in this context particularly in explaining the motion of crack propagation while evaluating the deformation of the RC structures.

As far as finite element analysis is concerned, a lot of works mainly based on two-dimensional (2D) modeling of RC structure without reinforcements and based on various integral methods has been reported in different reputed journals in last few decades. Attempts were made to improve performance of 2D isoparametric element based formulation using reduced and selective integration schemes, B-bar method, additional incompatible modes, but to a few specific problems and also under certain conditions of mixed formulation. Cazzani et al.(2005) developed a four-node hybrid assumed-strain finite element derived within the framework of first order deformation theory, particularly for the analysis of laminated composite plates. All these attempts were made aiming at removing inherent difficulties (locking etc.) particularly in thin structures. Even these methods can only analyze certain specific problems where it is possible to study the behaviour of the structure with necessary simplification by adopting the assumptions of 2D analysis. In applications of 3D analysis, the standard quadratic 20-noded hexahedral element has been used, though it has high number of nodes involving a large number of degrees of freedom and necessitates large computational time. Since comparatively lower order elements have the advantages for 3D analysis due to easy mesh generation, data interpretation and lower computational time, improvement of such type of element performance has drawn attention of the investigators.

Among the lower order elements, the linear isoparametric elements are the simplest constant strain elements. However it has got some well-known deficiencies as far as the finite element analysis is concerned. It cannot represent the state of stress

in pure bending accurately due to inherent volumetric and transverse shear locking phenomenon. Earlier in this regard, methods were described to improve the performance of the standard linear quadrilateral and hexahedral elements with the introduction of additional imaginary incompatible degrees of freedom to represent different modes of deformation, of course those are condensed prior to the assembly of elements. Nowadays this difficulty with the associated locking phenomena has been overcome using a different concept of Enhanced Assumed Strain Approach (EAS) by Simo and Rifai (1990) in near incompressible and bending situations, where the strain field is enhanced with inclusion of additional variables. Numerous growth in this line have been reported in the literature by Simo and Armero (1992), Andelfinger and Ramn (1993), Souza et al. (1990), Cesar et al. (1999), (2002), Valente et al. (2002) and Murthy et al. (2007). Kim et al. (2004) developed a simple triangular solid element using an assumed strain field to alleviate the locking effect for the analysis of plates and shells. A remarkable progress and accuracy has been obtained by the EAS element HCiS18 introduced by Sousa et al. (2002), (2003) even with the coarser meshes and also successfully implemented in Samanta and Ghosh (2008a & b), (2009). In the present case, this element has been used to model the parent material i.e. concrete of the reinforced concrete structures as an extension in nonlinear regime to the previous work done by Samanta and Ghosh (2008a & b), (2009).

Another aspect of RC structure is that it is highly non-homogeneous due to discrete presence of the reinforcements. In general there are three methods available for modeling of reinforcement, e.g. the discrete, the smeared and the embedded approach. The first one represents reinforcements by truss elements those are connected to the mesh at the concrete/parent element nodes and hence finite element mesh generation becomes dependent on reinforcement layout. The second one (smeared) is more suitable for homogeneous or uniformly distributed reinforcements, such as wall panels. So they cannot be generally applied to 3D structures. Within embedded approach, proposed by Elwi and Hrudey (1989), Barzegar and Madipuddi (1994), these restrictions were removed and even the reinforcements are superimposed as one dimensional uni-axial element with the same displacement field as parent/concrete element without any additional node /DOF. They are allowed to intersect the parent element at any location and hence mesh design becomes independent of reinforcement layout. Here the author has used the same method proposed by Cheng and Fan (1993), Gomes and Awruch (2001) due to its simplicity to handle problems of 3D analysis of RC structures to model the reinforcement.

Accounting for interaction between parent material/concrete and the reinforcements are done to make RC structure to behave in a more realistic way because con-

crete is a strong, relatively durable in compression and reinforcements are strong, ductile in tension. This composite action requires transfer of load between concrete and steel. This load transfer mechanism is referred as bond-slip, which is depicted as continuous stress field in the vicinity of steel-concrete interface. As the loading on RC structures is gradually increased, this bond-slip effect increases and as a result equilibrium is set up in the domain with more relaxation of steel stress. To account for this phenomenon, two different approaches are very common. The first approach makes use of the bond-link element as proposed by Ngo and Scordelis (1967). This bond-link element has got no physical dimension and it connects a node of a concrete /parent material with that of a steel node having the same coordinate. It has been observed by the various authors that the bond-link element cannot adequately represent the stiffness of the steel concrete interface. The second approach makes use of bond-zone element described by a material law to model the contact surface between steel and concrete. Even though many studies of the bond-slip relationship between the mating surfaces have been conducted, a considerable uncertainty about this complex phenomenon still exists because of many parameters involved.

This phenomenon of interaction between the materials are modeled within the embedded approach where nodal D.O.F.s are increased by the slip D.O.F.s for each element and as a result global stiffness matrix size is increased dramatically. In bond behaviour, slip takes place due to damage in concrete adjacent to the bars exhibited by cracking /crushing. Lundgren (1999) developed an interface model based on plasticity theory with fully three-dimensional features. For all practical analysis of engineering problem, this approach is not very appealing, as it requires extremely large computational time. Another approach was initially introduced by Beer G. (1985) using isoparametric joint /interface element and was later on used by Hartl et al. (2000), Hartl and Elgamal (2000), Hartl and Beer (2000), where bond slip situations are being considered introducing supplementary interface elements of zero thickness. Within this approach, global displacement field is calculated at first considering perfect bond between reinforcements and concrete and then the slip is calculated by relaxing the perfect bond at the material level. Considering that many of the previous models and methods have not been fully verified so far, it is the intent of this study to address some of the model selection issues, in particular to the effect of bond-slip.

1.3 Scope and objective

In most of the earlier works of finite element analysis of reinforced concrete structures, emphasis has been given to predict load deformation characteristics either in terms of simplified 2D analysis in most of the cases or in terms of 3D analysis

using higher order elements. With the developments of science and technology in different areas individually, this paper simulates the elastic response of reinforced concrete beam considering (1) lower order solid elements which reduces time and associated cost in terms of easy and simple mesh generation together with data interpretation, (2) reinforcements as 1D truss elements considering only the axial deformation in its exact spatial position without affecting the parent element mesh in perfect bond situation following embedded approach, (3) mutual interaction between concrete and reinforcements for entire load history in terms of bond-slip phenomenon using continuous interface elements without affecting size of global stiffness matrix and (4) modeling of concrete considering both geometrical and material nonlinearity.

With the rapid growth in infrastructure throughout the world, it's very difficult to use and update the commercial softwares to cope up with new developments in technologies. Also they are not directly suitable to solve a problem in hand. Therefore, a substantial effort has been made to write simple finite element programs in the form of FORTRAN subroutines. The main emphasis has been given to understand the mechanics of concrete structures by considering both material as well as geometric non-linearity with appropriate failure criteria in an elegant way so as to minimize the gap between numerical solutions and experimental results. The proposed material model is based on orthotropic hypoelastic model developed by Balan et al. (2001). The directions of orthotropy are assumed to coincide with current principal stress directions according to the rotating smeared crack approach. The hypoelastic model is dissipative by nature and it doesn't consider any flow rule as such. Instead it is based on a fictitious equivalent uniaxial strain to take care of the entire deformation path during loading.

It is shown that the accuracy of the formulation in interpreting the response in this highlighted area is highly comparable to that of the existing analytical models. The present paper is an initial attempt on a continuing investigation of the finite element analysis of reinforced concrete members utilizing lower order solid hexahedral elements including assessment of the effect of reinforcement together with bond slip. Ultimate purpose of this research is to make feasible the detailed numerical study of the behaviour of the reinforced concrete members through their entire elastic and inelastic ranges using non linear material properties as well as failure criteria of concrete, of course incorporating tension stiffening and cracking phenomenon. Further, the utility of the analytical model may be verified from the extensive experimental investigations to establish its true potentiality.

2 Formulation

2.1 Concrete

Concrete consisting of hardened cement paste with aggregates embedded in it, is highly heterogeneous. As a result, its behaviour is very complex. In general, concrete is assumed to behave linearly elastic and orthotropic even in multi-axial stress states for all engineering purpose. The proposed model includes the effect of triaxial nonlinear stress-strain law, tensile cracking, compression crushing and strain softening under monotonic loading condition. As plain cement concrete undergoes large relative displacements, only small deformation has been accounted for along with rigid body rotations. Hence a total Lagrangian formulation has been followed although with engineering stress and strain in the finite element implementation. The total secant stiffness has been used for the incremental stress-strain relations to account for strain softening at higher stress levels.

2.1.1 FE Formulation

A classical isometric formulation is followed with three translational degrees of freedom at each node of 8-noded solid hexahedral elements to model the parent material (concrete) of the reinforced concrete. Using the standard elasticity matrix for the parent material D_P, strain displacement matrix B_P, 3D transformation matrix $T_{\sigma,gl}$, volume considered V_P, p being the subscript to denote the parent material and their usual interrelationships for the continuum in 3D stress state, the element stiffness is derived in a very straightforward way as ;

$$K_P^e = \sum_P B_P^T . \left[T_{\sigma,gl}^T \right] . D_P . \left[T_{\sigma,gl} \right] . B_P . dV_P . \tag{1}$$

The element stiffness matrix formulated thus can not infer about the internal stresses set up due to it's inability to represent the state of pure bending strains and due to fictitious inclusion of large shear strains. As a result, structural response (deflection) is grossly underestimated as well as become dependent on mesh design. An enhanced strain formulation proposed by Sousa et al (2003) is incorporated based on extra compatible modes of deformation which don't have physical meaning and are eliminated at the element level by static condensation method. In particular element is designated as HCiS18, where 18 nos. of new extra variables (α) are associated in addition to the usual strain displacement vector (ε_P) and the augmented strain displacement vector (ε'_P) becomes (with 'w' being the displacement field);

$$\left\{ \varepsilon'_P \right\} = \left\{ \varepsilon_P \right\} + \left\{ \varepsilon_\alpha \right\} = \begin{bmatrix} B_P & B_\alpha \end{bmatrix} . \begin{Bmatrix} w_P \\ w_\alpha \end{Bmatrix} \tag{2}$$

With $N_\alpha = \frac{1}{2}(1-\xi^2).(1-\eta^2).(1-\varsigma^2)$ as the bubble function, the enhanced strain matrix, B_α becomes

$$B_\alpha = \frac{|J_0|}{|J|}.T_0.B_\alpha^{18} \tag{3}$$

Where J_0 and J is the Jacobian determinant evaluated respectively at $\xi = \eta = \varsigma = 0$ and at each Gauss points, T is the transformation matrix and $\left[B_\alpha^{18}\right]$ is obtained from the Sousa et al. (2002, 2003). It is well established and has also proved its worth in evaluating the performance of the reinforced concrete structures in the present investigation.

The geometric nonlinearity is considered by modifying the usual strain-displacement matrix such that $B = B_0 + B_L$, where B_0 is the infinitesimal linear part and B_L is due to large deformation. The stiffness matrix is also modified such that $K = \bar{K} + K_\sigma$, where $\overline{K}$ is calculated using B_L and $K_\sigma = \int G^T.\sigma.G.dv$ such that

$$\sigma = \begin{bmatrix} S & 0 & 0 \\ 0 & S & 0 \\ 0 & 0 & S \end{bmatrix}$$

with

$$S = \begin{bmatrix} \sigma_x & \tau_{xy} & \tau_{xz} \\ \tau_{xy} & \sigma_y & \tau_{yz} \\ \tau_{xz} & \tau_{yz} & \sigma_z \end{bmatrix}$$

The strain-displacement matrix B_L due to large deformation is evaluated, as usual, in three dimension such that $B_L = A.G$ with $[A]$ as the matrix of displacement derivatives and $[G]$ as the geometric matrix using Crisfield (1997)

2.1.2 Material model

Concrete is considered as an isotropic material initially and then it becomes anisotropic during subsequent phases of loading. Accordingly the stress at each point is defined by three principal stresses and the concrete is considered as a nonlinear orthotropic medium with the direction orthotropy coinciding with the principal stress directions (Elwi and Murray (1979), Balan et al. (2001). In this approach, the incremental stress-strain relations of concrete in multiaxial stress state can be written as

$$\{d\sigma\} = [D_P].\{d\varepsilon\} \tag{4}$$

where $\{d\sigma\}$ and $\{d\varepsilon\}$ are the vectors stress and strain increments respectively and $[D_P]$ is the incremental concrete constitutive matrix with respect to the local or-

thotropic axes (1, 2, 3). By employing symmetry condition of the compliance tensor, the incremental stress-strain relationship of concrete in local coordinate system is expressed as

$$\begin{Bmatrix} d\sigma_1 \\ d\sigma_2 \\ d\sigma_3 \\ d\tau_{12} \\ d\tau_{23} \\ d\tau_{31} \end{Bmatrix} = \frac{1}{\Omega} \begin{bmatrix} E_1(1-\mu_{23}\mu_{32}) & E_1(\mu_{21}+\mu_{23}\mu_{32}) & E_1(\mu_{31}+\mu_{21}\mu_{32}) & 0 & 0 & 0 \\ E_2(\mu_{12}+\mu_{13}\mu_{32}) & E_2(1-\mu_{13}\mu_{31}) & E_2(\mu_{32}+\mu_{12}\mu_{31}) & 0 & 0 & 0 \\ E_3(\mu_{13}+\mu_{12}\mu_{23}) & E_3(\mu_{23}+\mu_{13}\mu_{21}) & E_3(1-\mu_{12}\mu_{21}) & 0 & 0 & 0 \\ 0 & 0 & 0 & G_{12}\Omega & 0 & 0 \\ 0 & 0 & 0 & 0 & G_{23}\Omega & 0 \\ 0 & 0 & 0 & 0 & 0 & G_{31}\Omega \end{bmatrix} \begin{Bmatrix} d\varepsilon_1 \\ d\varepsilon_2 \\ d\varepsilon_3 \\ d\gamma_{12} \\ d\gamma_{23} \\ d\gamma_{31} \end{Bmatrix} \quad (5)$$

where i =1, 2 and 3 stands for axis of orthotropy; $d\varepsilon_i$ = normal strain increment in ith direction and $d\gamma_{ij}$ = shear strain increment in plane i-j; $d\sigma_i$ = normal stress increment in ith direction; $d\tau_{ij}$ = shear stress increment in plane i-j; μ_{ij} = Poisson's ratio in ith direction due to stress in jth direction; $\Omega = 1-\mu_{21}\mu_{12}-\mu_{31}\mu_{13}-\mu_{23}\mu_{32}-\mu_{12}\mu_{23}\mu_{31}-\mu_{21}\mu_{32}\mu_{13}$; E_i = total secant modulus in the ith direction of orthotropy; G_{ij} = total secant shear modulus in plane i-j assumed as invariant under the transformation of coordinates, expressed as

$$G_{ij} = \frac{E_i.E_j}{E_i(1+\mu_{ij})+E_j(1+\mu_{ji})} \quad (6)$$

Since $[D_P]$, the incremental concrete constitutive matrix is defined w.r.t. the local orthotropic axes, the same has to be transformed to the global coordinate system before element stiffness matrix is formed using the standard 3D transformation matrix. For the incremental concrete constitutive matrix defined in Eq. (5), the evaluation of nine incremental modulli uses the concept of equivalent uniaxial strain (ε_{ui}).

Uniaxial Stress-Equivalent Strain Relation

A uniaxial concrete law is required to obtain the stress corresponding to ε_{ui}.Kwon and Spacone (2002), Balan et al. (2001) propose to use the Popovics' curve upto the peak compressive stress under monotonic loading. It assumes that the actual stresses are the functions of the current equivalent uniaxial strains, which are calculated based on the actual strain increments. For ($\varepsilon/\varepsilon_c$)<1 i.e. compressive ascending region of concrete, the law (for i = 1, 2, 3) is defined by

$$\sigma_i = R_{ci}.\frac{K_i.\left(\frac{\varepsilon_{ui}}{\varepsilon_{ci}}\right)}{1+A_i.\left(\frac{\varepsilon_{ui}}{\varepsilon_{ci}}\right)+B_i.\left(\frac{\varepsilon_{ui}}{\varepsilon_{ci}}\right)^2+C_i.\left(\frac{\varepsilon_{ui}}{\varepsilon_{ci}}\right)^3} \tag{7}$$

where R_{ci} = Concrete strength in i^{th} direction at current principal stress ratio; ε_{ci} = Corresponding equivalent uniaxial strain and the remaining constants (K_i, A_i, B_i, C_i) are found in Balan et al. (2001).

For ($\varepsilon/\varepsilon_c$)>1 i.e. compressive descending region of concrete, the stress is reduced linearly and concrete is assumed to crush if any point reaches at ultimate stress $R_{fi}(= k.R_{ci})$as shown in Fig.-1. The ultimate stress of concrete was assumed to be R_{fi} = $0.75R_{ci}$and the corresponding ultimatestrain was .00399. The required incremental secant modulus (for i = 1, 2, 3) could be determined directly dividing Eq. (7) by ε_{ui} according to Balan et al. (2001) as;

$$E_i = \frac{E_0}{1+A_i.\left(\frac{\varepsilon_{ui}}{\varepsilon_{ci}}\right)+B_i.\left(\frac{\varepsilon_{ui}}{\varepsilon_{ci}}\right)^2+C_i.\left(\frac{\varepsilon_{ui}}{\varepsilon_{ci}}\right)^3} \tag{8}$$

For descending branch of the proposed curve in Fig.-1, E_{soft} has been evaluated based on Rabezuk et al. (2005) to account for strain softening during compressive loading.

Poisson's ratio

It is necessary to define the variation of Poisson's ratio for implementation of the model. As suggested by Chen (1982), the variation of Poisson's ratio is negligible until the stress level reaches almost 80 percent of the compressive peak stress (R_{ci}) in the ascending branch of the stress-strain curve. As the stress level further increases till it reaches R_{ci}, a subsequent volumetric expansion of concrete takes place due higher value of strain. For this region, the following expression is used to describe the variation of the Poisson's ratio, as given by Balan et al. (2001);

$$\mu_{ij} = \sqrt{\mu_{ui}.\mu_{uj}.\frac{E_i}{E_j}} \quad (i = 1,2,3) \tag{9}$$

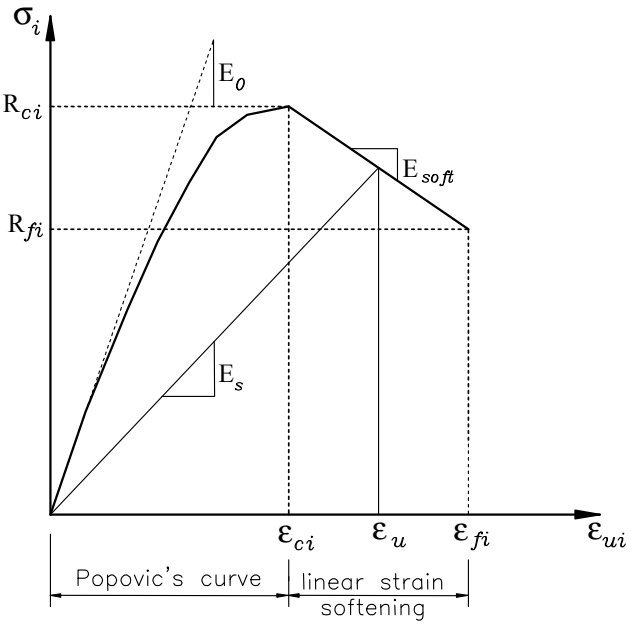

Figure 1: Monotonic Stress-Equivalent Uniaxial Strain Curve of Concrete

where μ_{ij} = Poisson's ratio (for i = 1, 2, 3) defined as function of cubic function of equivalent uniaxial strain as

$$\mu_{ui} = \mu_0 \left[1 + A_i . \left(\frac{\varepsilon_{ui}}{\varepsilon_{ci}} \right) + B_i . \left(\frac{\varepsilon_{ui}}{\varepsilon_{ci}} \right)^2 + C_i . \left(\frac{\varepsilon_{ui}}{\varepsilon_{ci}} \right)^3 \right] \tag{10}$$

where μ_0 = initial Poison's ratio and other parameters are the same as defined earlier except $K_i = 1/2\mu_0$. For the stress level R_{ci}, μ reaches almost a constant value of 0.36 and remains constant till concrete reaches the breaking stress due to dilatancy phenomenon.

The proposed model is based on the concept of equivalent uniaxial strain and are defined on material axis of orthotropy, which is assumed to coincide with the direction of principal stress at each load step. For three-dimensional problems, the principal stresses and the associated directions are evaluated mathematically as eigenvalues and eigenvectors of σ in a way also shown in Boresi and Sidebottom (1985).

Ultimate Surface

The evaluation of the incremental secant moduli in Eq. (8) also requires the determination of the parameters involved in it. These parameters vary with the principal

stress ratio and hence are determined by defining a surface in the principal stress space. Such a surface, which defines ultimate values of strength or strain for a particular stress ratio is termed as 'failure surface'. This failure surface is more appropriately called as 'ultimate strength surface' in this case as it also takes care of strain softening of the material. Choosing 'ultimate strength surface' for material like concrete is very crucial for prediction of its behaviour under complex multiaxial stress state. The ultimate strength surface of concrete due to multiaxial stress state is described in this presentation by considering the five parameter surface originally proposed by Argyris, later on modified by Willam and Warnke for high compression zone [Chen (1985)]. In connection with three-dimensional incremental model for describing the nonlinear behavior of concrete, this five-parameter model considers the curved meridians using second order parabolic expressions and non-circular trace in the deviatoric plane using an elliptical curve. As a result, it has a smooth surface with unique gradient and continuous derivative everywhere and becomes valid for all stress combinations in the range of most practical applications including tensile stresses .The surface is defined by the following equation ;

$$\frac{F}{f_{cu}} - S \geq 0 \tag{11}$$

where, F is a function of the principal stress state (σ_{xp}, σ_{yp}, σ_{zp}).

$$F = \frac{1}{\sqrt{15}} \left[(\sigma_1 - \sigma_2)^2 + (\sigma_2 - \sigma_3)^2 + (\sigma_3 - \sigma_1)^2 \right]^{1/2} \tag{12}$$

$S =$ failure surface expressed in terms of principal stresses

$$= \frac{2r_2 \left(r_2^2 - r_1^2\right) .Cos\theta + r_2 \left(2r_1 - r_2\right) . \left[4 \left(r_2^2 - r_1^2\right) Cos^2\theta + 5r_1^2 - 4r_1 r_2\right]^{1/2}}{4 \left(r_2^2 - r_1^2\right) .Cos^2\theta + \left(r_2 - 2r_1\right)^2} \tag{13}$$

and five input parameters f_t, f_{cu}, f_{cb}, f_1 and f_2. f_t= ultimate uniaxial tensile stress, f_{cu}= ultimate uniaxial compressive stress, f_{cb} = ultimate biaxial compressive stress, being f_1 = the ultimate compressive stress point for a state of biaxial compression on tensile meridian and f_2 = the ultimate compressive stress point for a state of biaxial compression on compressive meridian. However this failure surface is defined in terms of two parameters viz. f_t, f_{cu} and the rest three parameters are expressed in terms of f_{cu}.

Both the function 'F' and failure surface 'S' are expressed in terms of the principal stresses denoted as σ_1, σ_2 and σ_3 where, σ_1 = max (σ_{xp}, $\sigma_{yp,}\sigma_{zp}$), σ_3 = min (σ_{xp},

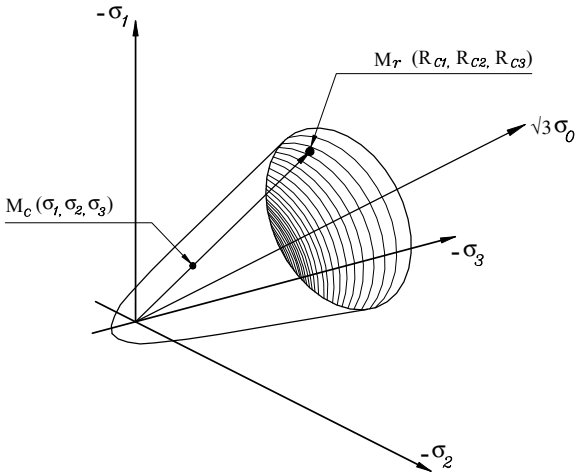

Figure 2: Concrete Failure Surface and Current Material Strength

σ_{yp}, σ_{zp}) and $\sigma_1 \geq \sigma_2 \geq \sigma_3$. The terms used to define 'S' are

$$Cos\theta = \frac{(2\sigma_1 - \sigma_2 - \sigma_3)}{\sqrt{2}\left[(\sigma_1 - \sigma_2)^2 + (\sigma_2 - \sigma_3)^2 + (\sigma_3 - \sigma_1)^2\right]^{1/2}}$$

$r_1 = a_0 + a_1\xi + a_2\xi^2$ and $r_2 = b_0 + b_1\xi + b_2\xi^2$ with $\xi = \sigma_h / f_{cu}$ and $\sigma_h = (\sigma_1 + \sigma_2 + \sigma_3)/3$. The values of the undetermined coefficient $a_0, a_1, a_2, b_0, b_1, b_2$ may be found from the reference Elwi and Murray (1979) using the nondimensional values of the tensile and biaxial compression strength as $\alpha_t = f_t / f_{cu}$ and $\alpha_c = f_{cb} / f_{cu}$. Similarly, for the evaluation of the ultimate equivalent uniaxial strains ε_{ci} corresponding to ultimate strength R_{ci}, there exists a surface in the equivalent uniaxial strain space that has the same form as the ultimate strength surface defined earlier. This surface is defined by replacing σ_1, σ_2, σ_3, f_t and f_{cu} in Eq. (11) by ε_{u1}, ε_{u2}, ε_{u3}, ε_t and ε_{cu}respectively.

The current concrete strength values R_{ci} (i=1 to 3) are determined from the ultimate strength surface. For the current stress level, first the corresponding principal stress values σ_i (i=1 to 3) are calculated. A point M_c (σ_1, σ_2, σ_3) is considered in the principal stress space and then a line that extends from origin through M_c intersects the ultimate strength surface at $M_r(R_{c1}, R_{c2}, R_{c3})$, where R_{ci} is the required current concrete strength of concrete in the i-direction. Here this concept has been utilized to find R_{ci}, but with reference to the rendulic plane as proposed by Elwi and Murray (1979), Bouzaiene and Massicote (1997). Also the parameters σ_{fi} and ε_{fi}, on the

descending branch of the stress-equivalent strain curve in Fig.-1 are to be supplied in order to calculate incremental moduli defined in Eq. (8). Since these two parameters controls the nature of descending branch and vary from case to case indicating thereby highly test dependent, it is assumed as proposed by Balan et al. (2001) ;

For compression loading: $\sigma_{fi} = 0.85.R_{ci}$ and $\varepsilon_{fi} = 1.41.\varepsilon_{ci}$.

For tension loading: $\sigma_{fi} = 0.25.R_{ci}$ and $\varepsilon_{fi} = 4.0.\varepsilon_{ci}$.

Concrete in tension

Nonlinear behaviour of concrete is characterized by formation and propagation of tensile cracks. To model the cracking behaviour of concrete under tensile stress, smeared crack approach is considered. According to the smeared crack approach, cracking of concrete is assumed to form at the integration points of the finite element in a plane perpendicular to the direction of maximum principal tensile stress as soon as this tensile stress reaches the specified tensile strength. Once a crack is formed, the behaviour of concrete at that integration point becomes orthotropic and it continues to remain for that load step. New crack directions are considered to be initiated at a different load step.

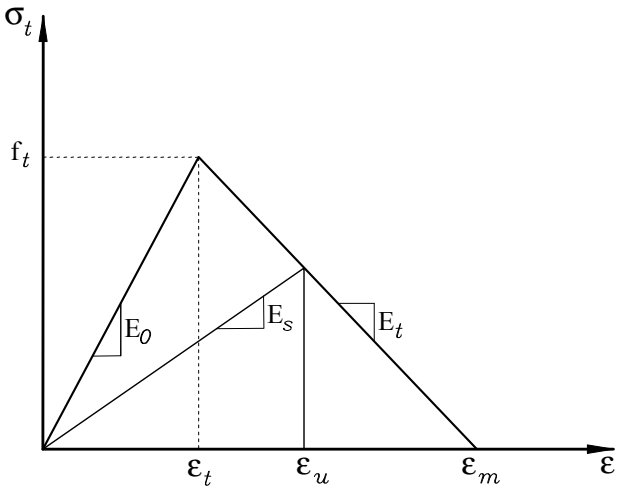

Figure 3: Linear strain softening model of concrete in tension

After concrete cracking, tensile stress is not immediately set to zero but is gradually released by a linear strain softening behaviour as in Cho and Hotta (2002). The total strain increment consists of two parts: the concrete strain increment and the crack strain increment. The strain softening modulus E_t is derived as fracture energy of

concrete as follows.

$$\frac{1}{E_t} = \frac{1}{E_0} + \frac{1}{C_{cr}} \tag{14}$$

where, cracking modulus $C_{cr} = -\frac{f_t^2.w_f}{2.G_f}$, w_f = crack band width and G_f = fracture energy of concrete required to produce one unit of area of a continuous crack.

It has been observed from various experimental data that after formation of a crack, sufficient shear stress could be transferred across the rough surfaces of cracked concrete due to aggregate interlocking and reinforcement ratio. A common practice to consider this phenomenon in a smeared crack model is to attribute an appropriate value to cracked shear modulus G_c in terms of uncracked shear modulus G with an appropriate shear retention factor, which has been followed by many researchers. In present study, an approach similar to Cho and Hotta (2002) has been adopted, where cracked shear modulus is assumed to reduce linearly as a function of current tensile strain (εp when it exceeds tensile strain (ε_t).

$$G_c = \alpha_c.G\left(1 - \frac{\varepsilon}{\varepsilon_m}\right), \text{ for } \varepsilon_t \leq \varepsilon \leq \varepsilon_m \tag{15}$$

Where α_c is used as 0.5 for one crack, 0.25 for more than one crack and ε_m is used as 0.004.

When a crack is formed, the material stiffness is reduced in the failure plane in the direction normal and parallel to the crack and the Poisson's ratios (μ_{12} and μ_{31}) become equal to zero in the crack plane and the stress normal to the crack is equal to zero. Thus the material starts to strain soften in the principal stress direction. Gradually σ_1 reduces to zero and the material looses stiffness in that direction. In this light, the generalized stress-strain relation defined in Eq. (3) needs to be modified for cracked concrete with the value of μ_{12} and μ_{31} equal to zero. When σ_1 becomes equal to zero, the corresponding diagonal term is actually equal to zero. However to avoid the numerical difficulty, the same element in the constitutive matrix is provided with a small value equal to unity.

Compression crushing

The above procedure is set to identify the failure due to the cracking phenomenon in the tensile regime. However under multi-axial stress condition, compression crushing may also take place, which is identified with the help of ultimate strength envelope as the current stress level reaches ultimate compressive strength R_{ci}. With reference to the Fig.-1, the descending branch of the curve during strain softening is considered as linear. As the material reaches the peak value of stress level at the onset compression crushing, strain softening in all direction start until minimum

stress reaches a value equal to σ_{fi}. With the assumption that Poisson's ratio μ_{ij} is equal to zero after compression crushing, the constitutive relation takes the form with only diagonal terms. In this situation, E_i the total secant modulus at the descending branch of the stress strain curve as shown in Fig.-1, may be calculated as proposed by Rabczuk (2005) ;

$$E_i = \frac{\sigma_{ci}}{\varepsilon_{ui}} + E_{soft} \cdot \left(\frac{\varepsilon_{ui} - \varepsilon_{ci}}{\varepsilon_{ui}} \right) \tag{16}$$

where, E_{soft} is the softening modulus of concrete in the descending portion of the curve, which in again may be calculated based on the ultimate values of stress and strain parameters.

2.1.3 Reinforcements

The reinforcement represents a discontinuity of the stiffness distribution within a reinforced concrete member. When such a domain is discretised by finite elements, only in a few situations the domain is subdivided to take care of the stiffness of the reinforcements in position appropriately. Hence a formulation is needed to account both concrete and reinforcement in an implicit manner.

2.1.4 FE Formulation

In this study, the straight reinforcement bars are modeled utilizing classical embedded approach proposed by Elwi and Hrudey (1989), Cheng and Fan (1993) and Hartl et al. (2000), where the same displacement field of the parent element is assigned. It allows discrete presentation of reinforcements at their exact spatial position without increasing the size of the global stiffness matrix if the perfect bond is assumed. In fact this approach may also be extended in bond-slip situations without increasing the parent element nodes as well as element stiffness matrix.

The reinforcements are embedded into the parent concrete element. Hence in the structural domain, the reinforcement layout remains independent of element mesh. The only requirement is to identify the elements with reinforcement(s) and their sectional properties together with its orientation, which may be taken care of by a preprocessing subroutine. The reinforcement nodes are generated independently of the element nodes within the respective element. The obtained strain field applies to the parent elements and to the reinforcement elements. Once it is identified it becomes very simple to handle problems of three-dimensional RC structures in perfect bond situations. Since the reinforcement nodes do not introduce additional degrees of freedom to the vector of nodal parent element displacements, size of the stiffness matrix remains unaltered.

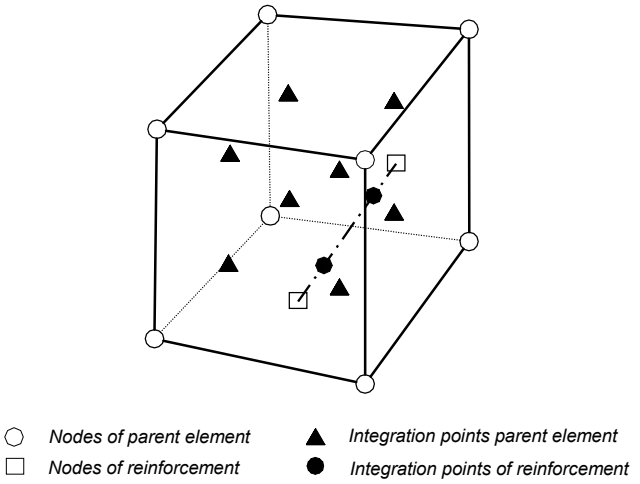

Figure 4: Parent element embedded with reinforcements

The stiffness of the reinforcements is calculated as one-dimensional elements embedded in the space of parent element and is then super-imposed on the stiffness of the parent element. The same strain displacement matrix B_P (used for the parent element) is utilized to evaluate the stiffness of the reinforcements. Since the reinforcement is considered as one-dimensional, the stiffness (integration) is to be evaluated along the path of the reinforcement(s). In order to integrate the stiffness contribution of the reinforcement(s) the strain displacement matrix has been computed at the respective gauss point(s) of the reinforcements expressed in terms of the intrinsic coordinates of the parent element. A Newton root finding algorithm in 3D is used for this purpose, where the known integration points of reinforcement in global coordinates are computed in local coordinates using an inverse mapping procedure based on iterative method by Barzegar and Madipuddi (1994). Thus the stiffness contribution of reinforcement towards the element becomes

$$K_R^e = \sum_{RB} B_P^T . T_{\varepsilon,gl}^T . D_R . T_{\varepsilon,gl} . B_P . dV_R, \tag{17}$$

Where RB is the number of reinforcement elements within the parent element and R is the subscript used to denote reinforcement. D_R is the elasticity matrix for the reinforcement due to uniaxial tension /compression in local coordinates with E_s as the initial modulus of elasticity of reinforcement $= 5000\sqrt{f_{cu}}$ in MPa. Once the integration points within the local coordinates are known, the composite element

stiffness matrix may be computed simply by adding Eq. (1) and Eq. (15) in perfect bond situation.

2.1.5 Material model

Unlike concrete, the properties of reinforcing steel are generally not dependent on environmental conditions and hence are considered as much durable than the concrete. Hence a single stress-strain diagram is adequate to define the material properties required for the sake of analysis of reinforced concrete structures in all possible load ranges [Kwak et at. (1997)]. For all practical engineering purposes, steel exhibits the same stress-strain curve both in tension and compression. In general, it shows linear elastic portion, a yield plateau and a strain hardening range in which stress again increases with strain and finally, the stress drops at the breaking point as shown in Fig.-5.

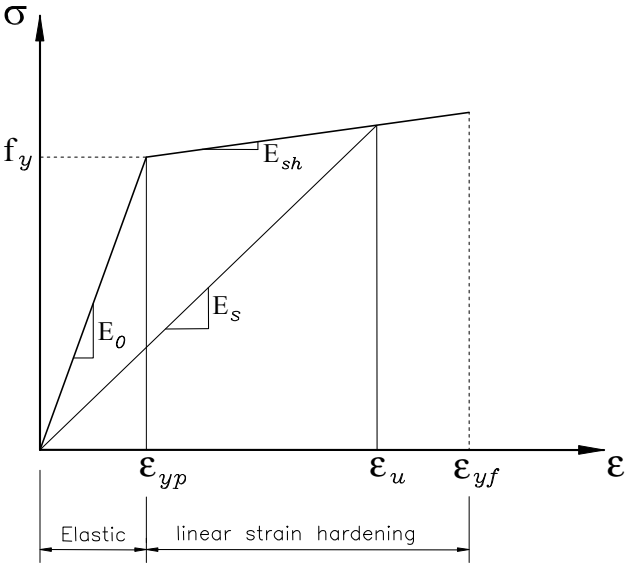

Figure 5: Steel stress-strain relation

The first idealization neglects the strength increase due to strain hardening and it is modeled as a linear material till the yield point as per various codes of national and international codes of practice. The second idealization of linear strain hardening is particularly useful for achieving numerical convergence /stability. Thus it is particularly useful for computational convenience and also the behaviour of RC members are not greatly affected by when the structure is loaded monotonically.

The following equations are being utilized here to determine secant modulus for the corresponding strain ranges ; $E_s = E_0$, for $\varepsilon \leq \varepsilon_{yp}$ and $E_s = \frac{f_y}{\varepsilon_u} + \frac{(\varepsilon_u - \varepsilon_{yp}).E_{sh}}{\varepsilon_u}$, for $\varepsilon_{yp} \leq \varepsilon \leq \varepsilon_{yf}$.

2.2 Modeling of Interface and Bond-Slip

Forces of interaction between concrete and reinforcement are transferred by bond due to chemical adhesion, friction and mechanical interaction at the interface. Deformed bars have better bond than plain bars due better mechanical interlocking with the rough surface. Since bond stresses in reinforced concrete structures vary greatly due to change in the value of steel stresses along the length, it becomes very pronounced at the end anchorages as well as in the vicinity of cracks and hence controls the behaviour of RC members particularly subjected to higher stress levels. Most interestingly perfect bonding is not true throughout the loading history of a reinforced concrete structures. At the interfaces of high stress transfer, bond stress is related to the relative movement between the mating surfaces due to the presence of the cracks. Practically, strain compatibility remains no longer valid at such situations. This incompatibility and associated crack propagation gives rise to relative displacement between steel and concrete which is better known as bond-slip. However, at lower stress levels when it behaves elastically, a simplified analysis of RC structures may suffice assuming a rigid /perfect bond in between the two. In fact, perfect bonding of the reinforcements with the concrete over-predicts the shear transfer and this lead to an over or under estimation of the response of the structure depending on specific situation. Since it is the objective of the study to investigate the bond-slip behaviour of reinforcing steel in more detail, a more sophisticated bond-slip model RC structure is used in the formulation under monotonic loading.

2.2.1 FE Formulation

In finite element method, bond-slip is modeled in a conventional way by means of interface elements. In this respect, bond-link element was introduced by Ngo & Scordelis (1967) at first, later on bond-zone element was introduced by Groot and subsequently contact elements by Mehlhorn. The literature review recommends to modify the constitutive law of either concrete or reinforcements. Hardly any bond-slip model is available in the literature assigning same displacement field to both concrete as well as reinforcement and without increasing the size of the global stiffness matrix within the embedded approach.

Beer G. (1985) introduced an elegant way of continuous interface element and subsequently by Hartl et al. (2000), where bond-slip is accounted for at the material level by introducing supplementary interface elements between reinforcement and concrete after the displacement field has been computed based on rigid bond con-

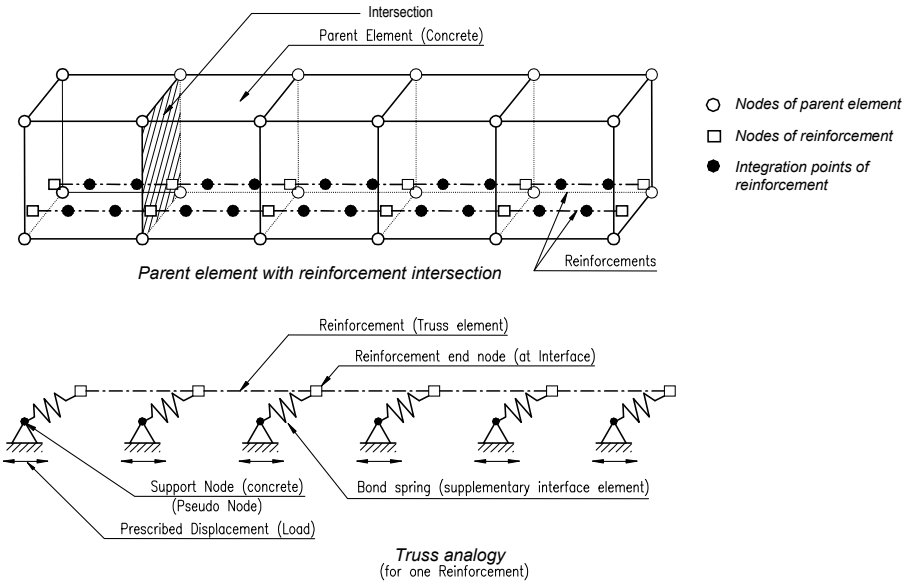

Figure 6: Supplementary Interface model

dition. Then the steel stress is relaxed due to bond-slip. The basic concept of supplementary slip algorithm is similar to that of a truss analogy as shown in Fig.-6, when the reinforcements are embedded in a classical way in the parent element without slip D.O.F. The truss members are the reinforcements and the supports are the concrete. The end points of the reinforcements are connected to the pseudo node on the concrete treated as support by bond spring, which are considered as continuous interface elements. Once the global displacement field is known, the strains along the reinforcement may be integrated and the same are referred as prescribed displacement of the supports. These support displacements get transferred to the end points of the reinforcements depending on the characteristic property of the bond spring. Thus the relative displacement of the reinforcement support node and the adjacent reinforcement end node is referred as bond-slip. The difference of the reinforcement force computed thus with respect to the same considering perfect bond are mapped back as residual nodal forces to the parent element.

In order to calculate slip, truss model is analyzed considering the stiffness of the reinforcement;

$$K_R^{=} A_R \sum_l B_R^T . E_S .. B_R . dl_R, \tag{18}$$

where, E_S is the secant modulus of reinforcements, B_R is the strain displacement

matrix for 1D reinforcement along its length $= \left[\frac{\delta N_1}{\delta S}, \frac{\delta N_2}{\delta S}\right] = \frac{1}{|J|} \cdot \left[\frac{\delta N_1}{\delta \xi}, \frac{\delta N_2}{\delta \xi}\right]$ and A_R is the cross sectional area of each reinforcements. The stiffness of the continuous interface element may be expressed as;

$$K_j = \sum_S B_j^T .k..B_j .dS \tag{19}$$

where, $B_j = \begin{bmatrix} N_1, & N_2, & -N_1, & -N_2 \end{bmatrix}$ is the strain-displacement matrix and k is the tangent modulus of interface element derived from bond-slip diagram depending on magnitude of slip. Once the stiffness of the reinforcement and the interface element is derived, they may be suitably placed in a matrix form as

$$\begin{Bmatrix} F_f \\ F_s \end{Bmatrix} = \begin{bmatrix} K_{ff} & K_{fs} \\ K_{sf} & K_{ss} \end{bmatrix} \cdot \begin{Bmatrix} u_f \\ u_s \end{Bmatrix}$$

where, $u_f = \begin{bmatrix} u_{1r} & u_{2r} \end{bmatrix}$ with 'f' as free node or reinforcement end node and $u_s = \begin{bmatrix} u_{1p} & u_{2p} \end{bmatrix}$ with 's' as support node or concrete node. It is to be noted that here an iteration is a must to obtain a convergent value of tangent stiffness as reinforcement-concrete interface behaviour is non-linear from the beginning of loading even when both concrete and steel remains in the elastic range. The end conditions are specified in terms of prescribed displacements (u_s) as Dirichlet boundary condition. Once these displacements at the free nodes (u_f) are calculated, the same set of equations are again solved for the revised slip until a good convergence is obtained with sufficient accuracy and then the relative displacements($u_{slip} = N_j^e .u_j^e$) of the nodes along with the steel stress due to bond slip are calculated. Finally this stress is mapped back as residual nodal forces of the respective parent element. Within this supplementary interface model, incremental strain update is inevitable. It is implemented by assuming linearly elastic behaviour of the reinforcements within the iterative scheme of the supplementary algorithm. As the slip converges to a stable solution, the stress in reinforcement is updated by the constitutive relation of the same.

2.2.2 Material model

The above supplementary slip algorithm may be effectively applied to incorporate the effect of bond-slip provided the value of the tangent modulus of interface element 'k' is available. Thus a bond stress versus slip relation is needed to implement the bond-slip algorithm. Various experimental investigations viz. ASTM pullout test among others suggest that the bond-slip relation depends on the position of reinforcements, the surface condition of bar, the loading state, the boundary condition i.e. the surrounding concrete, the confinement level and the anchorage length of the bar. In this study, a simple bond stress-slip model as per Modelcode-90 [MC90] is

adopted shown in Fig.-7, as it shows good approximation of the actual behaviour in cases of monotonic loading.

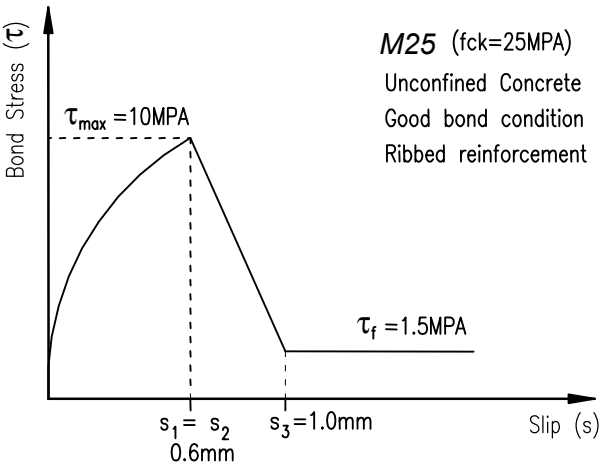

Figure 7: Bond-slip Relation

The monotonic envelope consists of an initial nonlinear relation due to adhesion stage in which the ribs of the deformed bars penetrate into the mortar matrix resulting in local crushing and microcracking. This ascending branch is given by

$$\tau = \tau_{\max} . \left(\frac{s}{s_1} \right)^{\alpha} \quad \text{for } 0 \leq s \leq s_1 = s_2 \tag{20}$$

where, α is parameter controls the curvature of the curve depending on the value of slip(s) and reflects reinforcement-concrete interface properties depending on bond condition and confined /unconfined concrete. The tangent modulus of the interface stiffness may be calculated by taking first derivative of the above equation as ;

$$k = \frac{\tau_{\max}}{s_1^{\alpha}} . \alpha . s^{\alpha - 1} \tag{21}$$

The second part of the curve τ decreases linearly to the ultimate value of frictional bond resistance (τ_f) due to reduction in bond resistance because of splitting cracks along the reinforcement upto s_3, i.e. residual bond capacity. In the present study, for deformed ribbed reinforcement in good bond condition for confined concrete the following values have been assumed ; $s_1 = s_2 = 0.6$mm, $s_3 = 1.0$mm, $\alpha = 0.4$, $\tau_{max} = 2.0\sqrt{f_{cu}}$ and $\tau_f = 0.3\sqrt{f_{cu}}$.

3 Solution algorithm

Although most of the finite element software, which are commercially available, have wide range of application, they do not offer adequate material models, also suitably integrated for response /stress analysis. In this part of the presentation, a brief description has been given mainly about the integration of the model elucidated previously. Here the initial stiffness approach is followed all along, during which the current stiffness matrix is formed only once at the beginning of each load step and also the crack direction remains unaltered during the entire load step. New crack direction are only assumed to form at subsequent load steps. It has also been assumed that since initially concrete does not show prominent nonlinearity during its uncracked elastic stage of loading approximately upto 25 percent of failure stress, no iterative solution is sought for two load steps at the very beginning of solution. For each problem, solutions are started with initial control parameters E_0, μ_0, f_{cu} and the material constants /parameters of the failure surface. In absence of any data modulus of elasticity of concrete is calculated by default as $E_0 = 5000.\sqrt{f_{cu}}$ and the same for reinforcement $E_s = 2.0E + 06$MPa. The various default parameters assumed are as follows;

- Various Strength Parameters of concrete (MPA)
  Ultimate uniaxial tensile strength $f_t = 0.10 f_{cu}$
  Ultimate biaxial compressive strength $f_{cb} = 1.15 f_{cu}$

- Various Strain Parameters (mm)
  Concrete
  Ultimate Uniaxial Compressive (Cracking) Strain ε_{cu}= 0.00283
  Ultimate. Uniaxial Compressive (Failure) Strain ε_{cm}= 1.41 ε_{cu}
  Ultimate Uniaxial Tensile (Cracking) Strain ε_t= 0.045 ε_{cu}
  Ultimate Uniaxial Tensile (Failure) Strain ε_m= 4.0 ε_t
  Ultimate Uniaxial Biaxial Compressive Strain ε_{cb}= 1.30 ε_{cu}
  Reinforcements
  Ultimate Uniaxial Tensile (yielding) Strain ε_{yp} = 0.0020
  Ultimate Uniaxial Tensile (Failure) Strain $\varepsilon_{yf} = 5.0\varepsilon_{yp}$

- Various Softening Modulii (MPa)
  With crack band width w_f = 15mm and fracture energy G_f = 180N/m,
  Softening Modulus of concrete in Tension E_{crack}= 822 Mpa
  Softening Modulus concrete in Compression $E_{soft} = 0.15 f_{cu}/0.41\varepsilon_{cu}$
  Softening Modulus of Reinforcement E_{sh}= $0.014E_0$

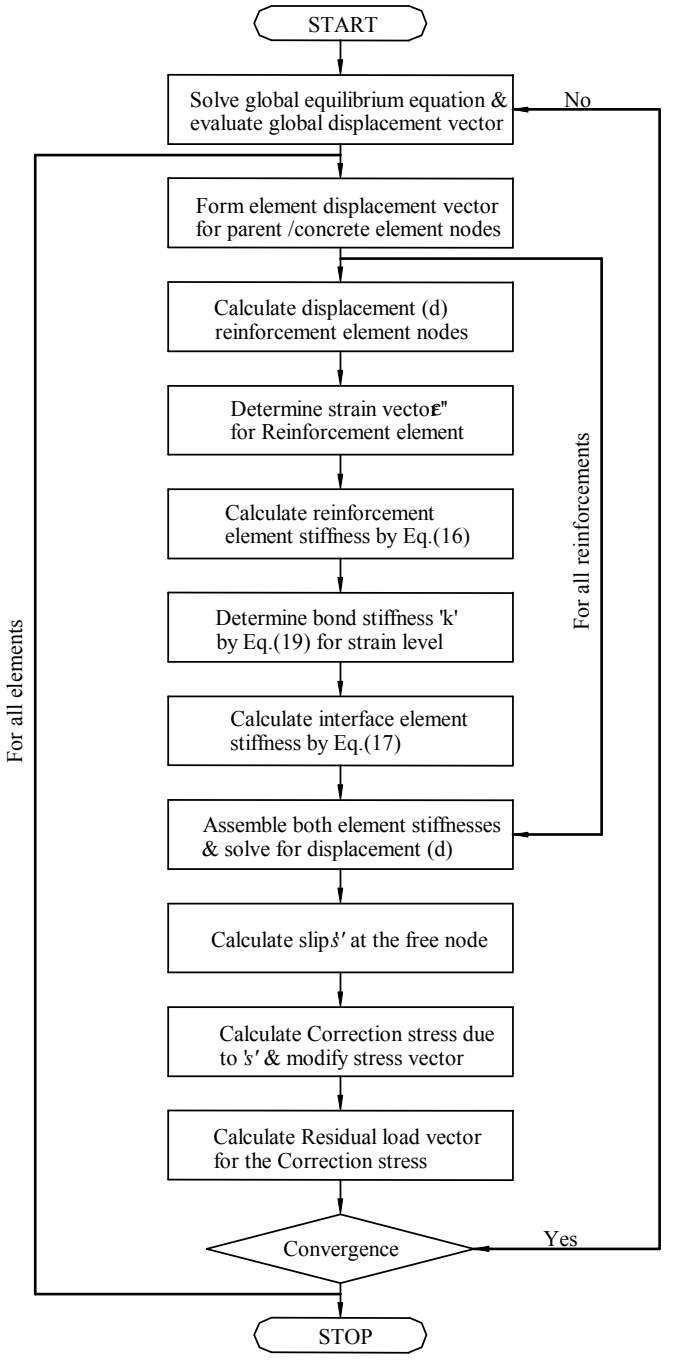

Figure 8: Solution algorithm for bond-slip model

Load steps are restricted to 10 percent of failure load in each case till crack initiation and later on it is reduced to 5 percent to avoid initiation of unrealistic numerical cracking. The incremental material constitutive matrix is calculated following specified stress path, as described by the model issues discussed earlier. The integrated element stiffness of concrete including contribution of reinforcement (if present in the parent element) is calculated at the beginning of each load step and the equilibrium equation is solved for using banded matrix solution. The criteria for the convergence of iterative solution within the load step is based the accuracy to satisfy global equilibrium equation or on the accuracy of determining total displacements. The failure load is assumed to occur at the load step, which requires higher number of iterations to satisfy equilibrium for convergence i.e. when it undergoes large strain under the applied load. In this study, maximum number of iterations was set to 30 and tolerance is 1.0 %. A flow diagram has also been included here (Fig.-8) to mention the procedure to execute the bond-slip model as discussed.

4 Case studies and discussion

In order to establish the potentiality of the model, a few benchmark examples (single span simply supported RC beam) have been taken from the literature and solved using the proposed model considering both material as well geometrical nonlinearity. The material nonlinearity is handled by hypoelastic formulation in three dimensions and the geometrical nonlinearity is taken care of by a Total Lagrangian formulation. The accuracy of the prediction in load-deflection response using the proposed model has also been checked different mesh density with and without considering bond slip.

The simple beam analyzed here is subjected to only uniformly distributed load (w) due to its own weight over the entire span along with point loads. The ordinary ribbed reinforcing steel (A_{st}) is placed at the bottom, which is in tension due to transverse loads. Provisions are not made to account for the effect of shear reinforcements. The concrete has the characteristic strength f_{ck}, which is assumed to be the same as ultimate uniaxial compressive strength f_{cu}. Both the parent material /concrete and the reinforcement are assumed to be initially linear elastic within first few load steps. With the supplied end points /profile of the reinforcements in the beam, the reinforcement mesh is also generated within each element for which stiffness contribution is added to the stiffness of the parent element. One of the main objectives was to assess the performance of the element HCiS18 in evaluating the response in bending situations considering incompressibility. To validate the integrated model proposed, comparisons have been made with experimental results of a few simply-supported beams from the literature. All these experiments

were performed to obtain better understanding of load-deflection behaviour of RC beams loaded to failure level primarily. The maximum load in the linear range has been considered as equal to 25% of the failure load as reported by the literature.

4.1 Beam # 1 : (RC-75-1, Shegg-Decanini, 1971)

This example model of simply-supported RC beam marked as RC-75-1 subjected to two point loads at quarter span tested by Shegg-Decanini(1971) was analyzed. The experimental results show the failure of this beam is due to yielding of tensile reinforcements, which was used by Gomes and Awruch (2001) for comparison. This beam has only two longitudinal tensile reinforcements, but has got no longitudinal compressive and transverse shear reinforcements.

The geometry, reinforcement details and its finite element mesh are illustrated in Fig.-9. The beam is 153mm by 246mm in cross-section, with a span between the simple supports of 3000mm. The beam is symmetrically loaded. The other parameters related to geometry are as follows d'' = 25mm, ω = 0.094 ton /m-run, E_{soft} = 6700 MPa and E_{crack} = 165 MPa. The magnitude of fracture energy is derived using the expression $\varepsilon_0 = \frac{2.G_f}{f_t.w_f}$. With tensile fracture strain $\varepsilon_0 = 0.013\%$ and values of f_t and w_f as above, G_f becomes equal to 210.0 N/m.

Based on experimental data, the following parameters related to geometry and material properties of concrete and reinforcements were considered; ultimate compressive strength f_{cu} =31.1 MPa, ultimate tensile strength f_t =2.15 MPa, initial modulus of elasticity E_0 =30,653 MPa, Poisson's ratio μ_0=0.15, area of reinforcement in tension A_{st} =235 mm^2, yield strength of reinforcement f_y =550 Mpa, shear modulus G_f =210 MPa and point load P =3.25 ton.

Four types of finite element mesh densities with 40, 48, 216, and 240 elements consisting of element size 153x123x150, 153x123x125, 76.5x82x83.3 and 76.5x82x75 respectively, were considered for the proposed numerical analysis to study the convergence criteria in regard to the element (HCiS18) and its behaviour considered in the proposed model. As the load-deflection diagram (Fig. 10) indicates that there is a large gap in predicting the response between Mesh-1, 2 and Mesh-3, 4 indicating thereby the effect of mesh density and the general applicability of coarse mesh using HciS18. In fact the response of Mesh-1 with 40 elements is still comparable and close to the experimental data. The contribution of bond slip is also not very significant in predicting the load displacement response of the system. In fact, in some of the load steps maximum deflection assuming perfect bond between concrete and reinforcement is similar to the same while relaxing the bond conditions. It is also important to note that the response of the system using the in-house code is better for coarser meshes, which uses the solid element HCiS18.

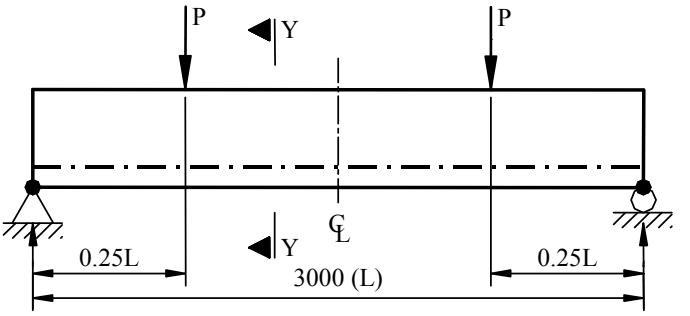

Experimental Configuration (Beam RC-75-1)
(Shegg & Decanini, 1971)

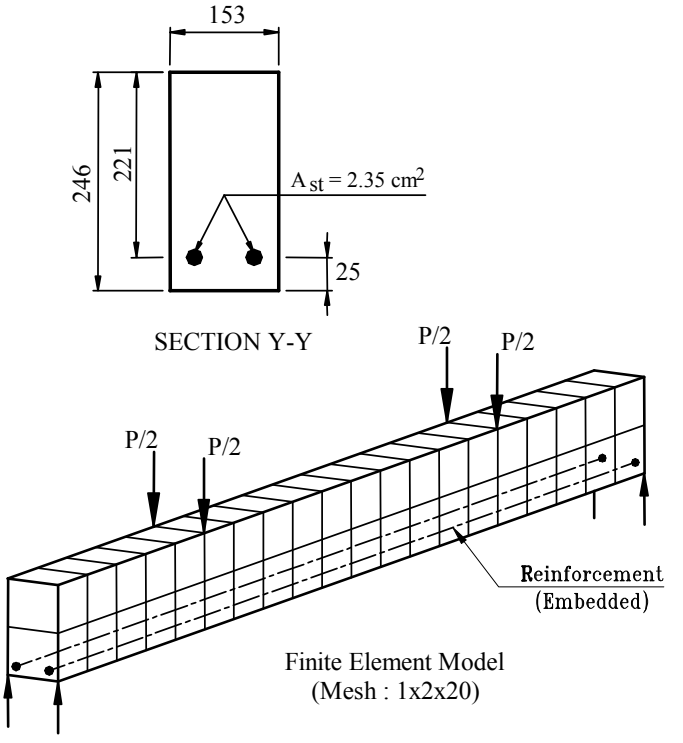

Figure 9: Details of RC beam (RC-75-1)

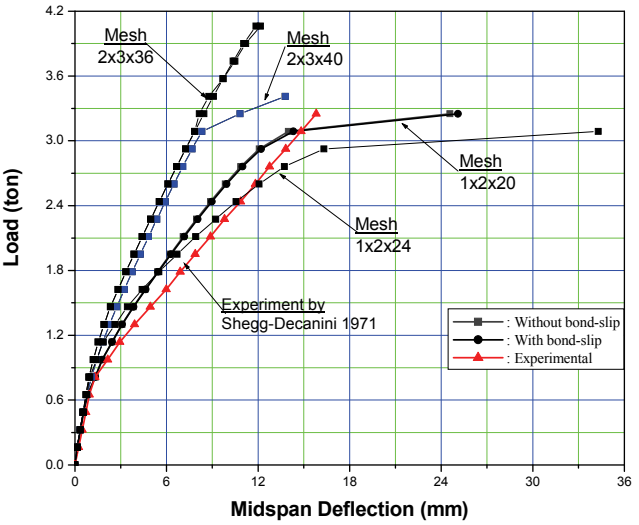

Figure 10: Comparison of Load-deflection response (RC-75-1)

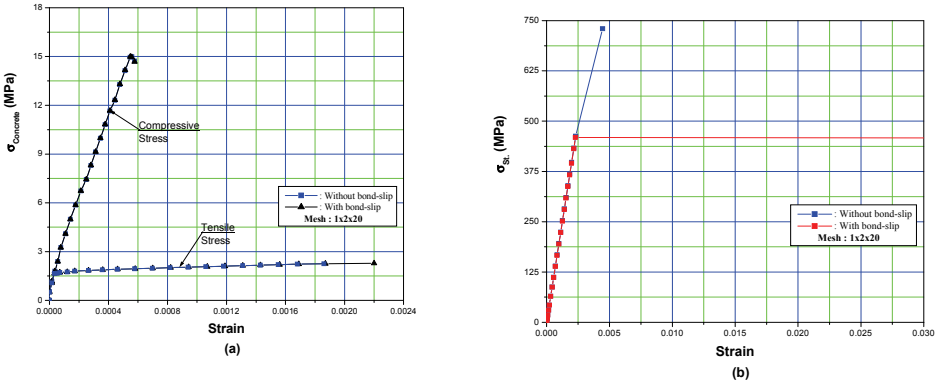

Figure 11: Stress-strain history (RC-75-1) using 40 elements (a) For concrete (b) For bottom reinforcement

The bending stresses (absolute values of both compressive and tensile) at the midspan of the beam has been plotted in Fig. 11. The non-linear material behaviour of concrete in compression may be noted. Also the tensile behaviour of concrete shows that the level of stress in tension is much lower compared to the same in compression and the stress value does change much beyond a very small value of strain in tension in concrete. The variation of stress in reinforcement in tension is

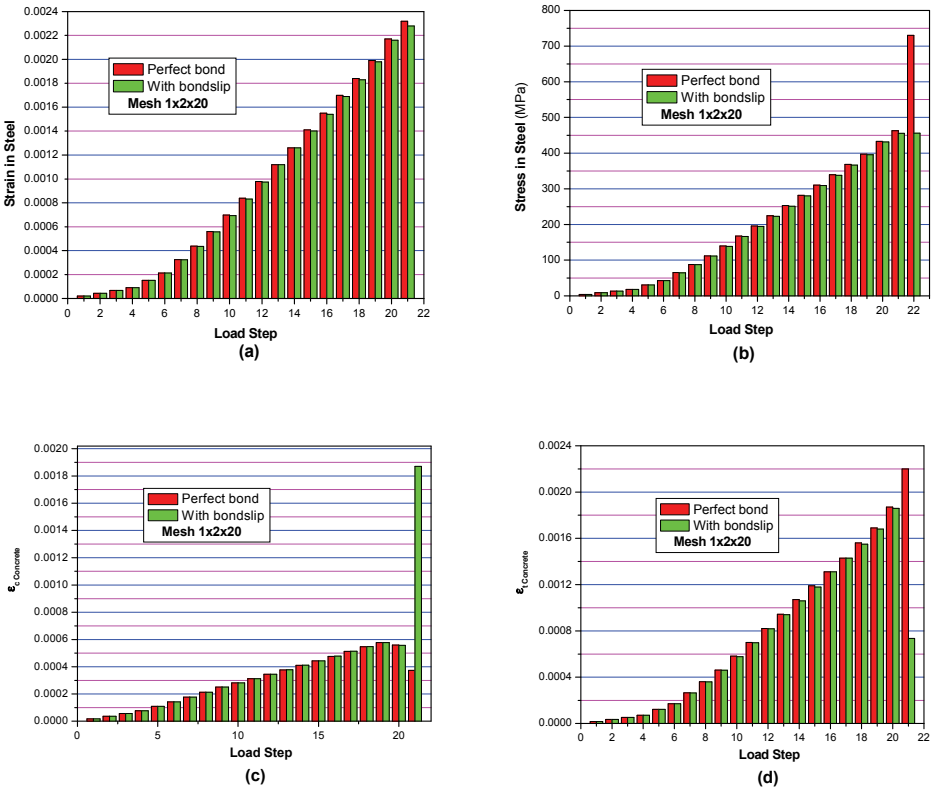

Figure 12: Effect of bond-slip (RC-75-1) using 40 elements (a) Strain in bottom reinforcement (b) Stress in bottom reinforcement (c) Compressive strain in concrete (d) Tensile strain in concrete

shown in Fig. 12. The yielding of reinforcement, obtained in case using the proposed model with bond-slip, is also supported by the numerical study performed by Gomes /Awruch (2001).

4.2 Beam # 2 : (Alvares, 1993)

This example model of simply-supported RC beam subjected to two point loads at quarter span, tested by Alvares (1993) was analysed. This benchmark experimental result was used by Oiliveira et. al. (2008) to validate the developed numerical model. This beam has three longitudinal tensile reinforcements and two longitudinal compressive reinforcements, but no transverse shear reinforcements. The geometry, boundary condition, reinforcement details and its finite element mesh are illustrated in Fig.-13. The beam is 120mm by 300mm in cross-section, with a

span between the simple supports of 2400mm. This study has been done to obtain the post-yield behaviour and capability of the model developed for the purpose.

The other parameters related to geometry are as follows ω = 0.09 ton/m-run, E_{soft} = 5495 MPa and E_{crack} = 175 MPa. The following parameters related to geometry and material properties of concrete and reinforcements were considered ; ultimate compressive strength f_{cu} =25.5 MPa, ultimate tensile strength f_t =2.044 MPa, initial modulus of elasticity E_0 =29,200 MPa, Poisson's ratio μ_0=0.17, area of reinforcement in tensionA_{st} =236 mm^2, yield strength of reinforcementf_y =500 MPa, E_s = 196,000 MPa and P =4.2 ton.

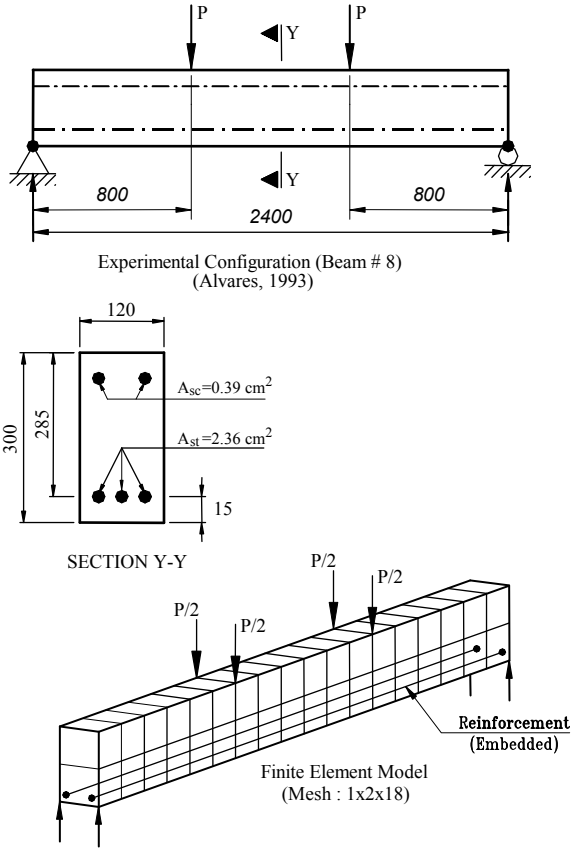

Figure 13: Details of RC beam (Alvares, 1993)

The alternatives of finite element mesh with 36 and 288 elements having element size 120x150x133.3 and 60x75x66.7 respectively were considered for the pro-

posed numerical analysis to study the convergence criteria in regard to the element (HCiS18) and its behaviour considered in the proposed model.

Fig. 14 shows the correlation between the measured load-deflection response of the beam and the proposed model. The results are presented with the above finite element mesh densities.

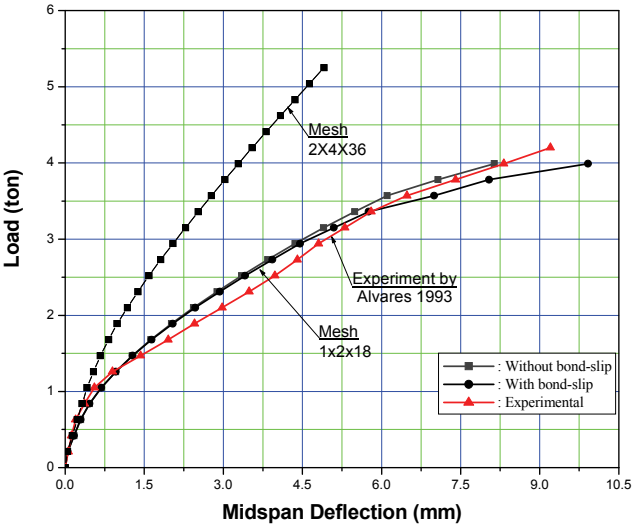

Figure 14: Comparison of Load-deflection response

The ratio of sides of the solid element may be consistently maintained close to 1.0 for better response. The response of test data shows that the sudden failure of the beam took place and it fails to pick up the definite yield plateau. In the analytical study, the main longitudinal reinforcements in compression were not considered. A satisfactory agreement between analysis and experiment was observed. As Fig. 5.3.3-2 clearly indicates that although the mesh is coarse one, the yielding and the failure of the beam fairly agrees with the experimental values.

Fig. 16(a) shows the variation of stresses both in compression fibre in the topmost layer as well as tension fibre in bottom-most fibre. Both the stresses are limited at perfect bond condition and less than the maximum value of stress considering bond-slip due to redistribution /relaxation of stress. Fig. 16(b) shows only the development of stresses in tensile reinforcements. In perfect bond condition, the maximum value of stress at failure is again less than the same while considering bond-slip. Of course, it is interesting to note that there is yielding of reinforcement predicted by this model, in case the effect of bond-slip is taken into consideration

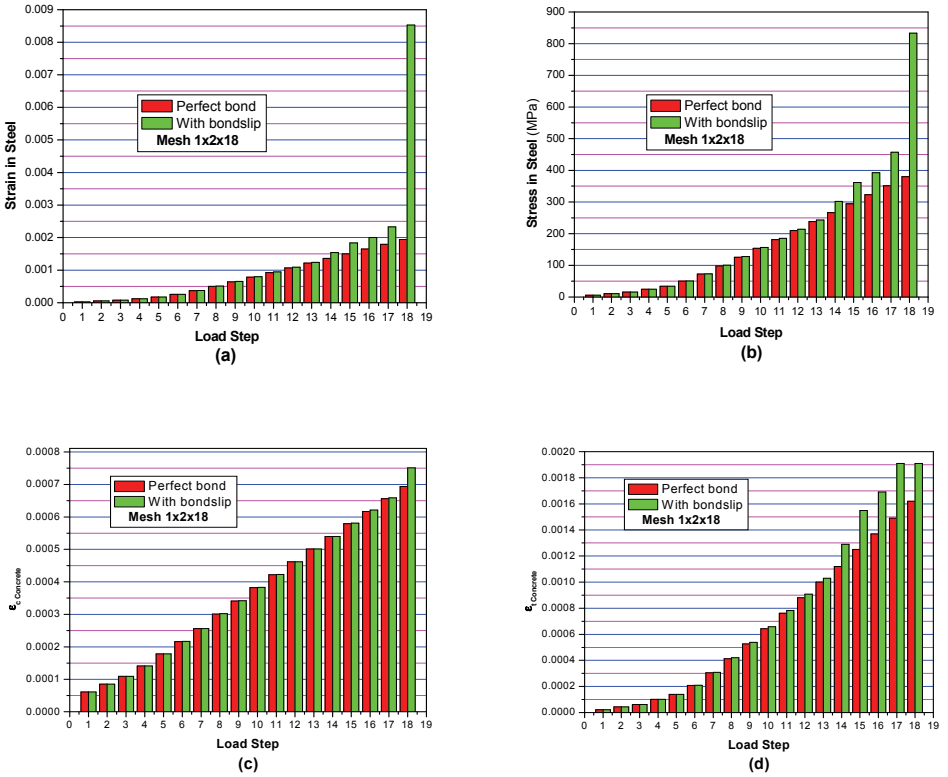

Figure 15: Effect of bond-slip (Alvares, 1993) using 36 elements (a) Strain in bottom reinforcement (b) Stress in bottom reinforcement (c) Compressive strain in concrete (d) Tensile strain in concrete

and it is also very similar to the assumed stress-strain diagram of steel in the proposed model. As noted in Fig. 15, the stress and strain of reinforcement as inferred by this model have been redistributed /increased due to bond-slip, also the tensile strain in concrete, but he compressive strain in concrete is not much affected by the same.

5 Conclusion and outlook

An integrated model for the analysis of simply supported RC beam based on standard linear hexahedral element has been presented, due to its simplicity in terms of easy mesh generation and data interpretation. Since this particular category of element exhibits some well-known deficiencies, it has been modified with the inclusion of enhanced strain modes. The performance of this new enhanced strain

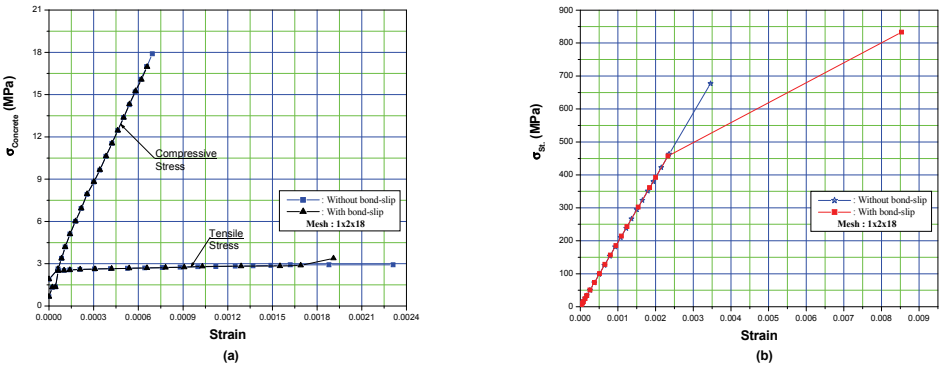

Figure 16: Stress-strain history (Alvares, 1993) using 36 elements (a) For concrete (b) For bottom reinforcement

element is very similar to the higher order element. It has been found that the modified lower order element is extremely efficient and effective in the analysis of three-dimensional problems. It may be inferred that the element in particular HCiS18 shows very good results even with coarser meshes, being almost accurate as best as the analytical case.

This model also includes the discrete presence of the reinforcement in arbitrary direction without affecting the parent element mesh. It has been shown that the concept of this FEM model (for incompressible situations) which includes the presence of the reinforcement in perfect bond condition and relaxed stress condition using bond-slip relation as given by the modelcode90 and its mathematical derivation is very simple and economical in terms of time consumption in terms of analysis efforts compared to other generalized methods. The validity of the formulation is verified by analyzing a few examples. It could be said that this model may work well for such reinforced concrete systems, where stiffness contribution of reinforcements are taken into account.

It has also been shown that the iterative scheme of the supplementary slip algorithm starts with the perfect bond predictions for reinforcement strains, which is obtained from the global solutions. Thus stresses are overestimated at the regions of the parent element domain, which experiences the highest strain. The approach causes no problem as long as stress in the reinforcement does not exceed the elastic limit within the iterative scheme. Since within the embedded approach, reinforcements are not restricted to the parent element nodes, the computational effort is reasonable. But when bond-slip is taken into account it requires higher time consumption. However this is becoming irrelevant with the availability of high-speed computers.

It has also been noted that the response as presented is not affected by the bond slip phenomenon at comparatively lower stress level, whereas the contribution of the same is much more pronounced at peak stress level as well as failure.

The program has been initially designed for reinforcements in tension zone only. No provision and attempt has been made to incorporate effect of reinforcement in compressive zone as well as presence of shear reinforcements. The development of the stresses in the stirrups may contribute well in performing gross response of the system, in particular at higher stress levels for doubly-reinforced sections. As such the developed program is only suitable for under-reinforced sections only. Hence an opportunity remains open for development with deeper emphasis in this direction also. The major limitation of the work is that it could not be implemented in a very general sense to all categories of reinforced concrete structure, as no experimental setup could be prepared during the span of the investigation work taken up for this purpose.

References

Andelfinger U., Ramm E. (1993): Analysis of 3D problems using EAS-elements for two-dimensional, three-dimensional, plate and shell structures and their equivalence to HR-elements. *Intl. Journal for Numerical Methods in Engineering,* vol. 36, pp. 1311-1337.

Balan T. A., Spacone E., Kwon M. (2001): A 3D hypoelastic model for cyclic analysis of concrete structures. *Engineering Structures*, vol. 23, pp. 333-342.

Balan T. A., Filippou F. C., Popov E. P. (1997): Constitutive model for 3D cyclic analysis of concrete structures. *Journal of Engineering Mechanics*, vol. 123, no.. 2, pp. 143-153.

Balakrishnon S., Murray D. W. (1988): Concrete Constitutive Model for NLFE Analysis of Structures. *Journal of Structural Engineering ASCE* , vol. 114, no. 7, pp. 1449-1466.

Barzegar F., Maddipudi S. (1994): Generating reinforcements in FE modeling of concrete structures.. *Journal of structural Engineering*, vol. 120,no. 5, pp. 1656-1661.

Beer G. (1985): An isoparametric joint/interface element for finite element analysis. *International Journal for Numerical Methods in Engineering,* vol. 21, pp. 585-600.

Boresi A. P., Sidebottom O. M. (1985): Advanced Mechanics of Materials. New York, *John Wiley & Sons Inc.*

Bouzaiene A., Massicotte B. (1997) Hypoelastic tridensional model for nonpro-

portional loading of Plain concrete. *Journal of Engineering Mechanics,* vol. 123, no. 11, pp. 1111-1120.

Cazzani A., Garusi E., Tralli A and Atluri S. N. (2005): A four-node hybrid assumed-strain finite element for laminated composite plates. *CMC: Computers, Materials & Continua,* Vol. 2, No. 1 pp. 23-38.

Cesar de sa J. M. A., Natal Jorge R. M. (1999) New enhanced strain elements for incompressible problems. *Intl. Journal for Numerical Methods in Engineering*, vol. 44, pp. 229-248.

Cesar de sa J. M. A., Natal Jorge R. M., Valente A. F. Robert and Arieas M. A. Pedro (2002): Development of shear locking-free shell elements using an enhanced assumed strain formulation. *International Journal for Numerical Methods in Engineering*, vol. 53, pp. 1721-1750.

Chen W. F. (1982): Plasticity in Reinforced Concrete. New York, McGraw Hill Inc.

Cheng Y.M., Fan Y. (1993): Modeling of reinforcement in concrete and reinforcement coefficient. *Finite Element analysis and design*, vol. 13, pp. 271-284.

Cho C.G., Hotta H. (2002): A study on compressive strength of concrete in flexural regions of reinforced concrete beams using finite element analysis. *Structural Engg. and Mechanics*, vol. 13, no. 3, pp. 1-15.

Crisfield M. A. (1997): Non-Linear Finite Element Analysis of Solids and Structures : Volume-I(Essentials) & Volume-II(Advanced Topics)', Chischester, UK, *John Wiley & Sons Ltd.*

Elwi A.E., Murray D. W. (1979): A 3d hypoelastic concrete constitutive relationship. *Journal of Engineering Mechanics div. ASCE*, vol. 105, no. 4, pp. 623-641.

Elwi A.E., Hrudey T. M. (1989): Finite element model for curved embedded reinforcement. *Journal of Engineering Mechanics*, vol. 115, no. 4, pp. 740-754.

Ferretti E., Di Leo A. (2008): Cracking and Creep Role in Displacements at Constant Load : Concrete Solids in Compression. *CMC: Computers, Materials & Continua*, vol. 7, no. 2, pp. 59-80.

Gomes H. M., Awruch A. M. (2001): Some aspects of three-dimensional numerical modeling of reinforced concrete structures. *Advances in Engineering software*, vol. 32, pp. 257-277.

Hartl H., Sparowitz L., Elgamal A. (2000): The 3D computational modeling of reinforced and prestressed structures. *Proceedings of the 3rd International PhD Symposium in Civil Engineering, Bergmeister K.(ed.*), *Vienna*, pp. 66-79.

Hartl H., Elgamal A. (2000): Non linear modeling of prestressed structures based on a continuum mechanics approach. *Heft 45 Osterreichische Vereinigung fur*

Beton-und Bautechnik,, Vienna, pp. 87-96.

Hartl H., Beer G. (2000): Computational modeling of reinforced concrete structures. *Festschrift zum 60, Geburtstag von Lutz Sparowitz, TU-Graz,* pp. 105-114.

Kim J. H., Kim Y. H., Lee S. W. (2004): An assumed strain triangular solid element for efficient analysis of plates and shells with finite rotation. *CMC: Computers, Materials & Continua,* Vol. 1, No. 2 pp. 141-152.

Kwon M., Spacone E. (2002): Three dimensional finite element analyses of reinforced concrete columns. *Computers and Structures*, vol. 80, pp. 199-212.

Kollegger J., Mehlhorn G. (1990): Material model for the analysis of reinforced concrete surface structures. *Computational Mechanics*, vol. 6, pp. 341-357.

Kwak H. G., Filippou F. C. (1997): Nonlinear FE analysis of R/C structures under monotonic loads. *Computers and Structures*, vol. 65, no. 1, pp. 1-16.

Kwak H. G., Kim S.P. (2001): Bond-slip behavior under monotonic uniaxial loads. *Engineering Structures*, vol. 23, pp. 298-309.

Lundgren K. (1999): Three-dimensional modeling of bond in reinforced concrete. Ph.D. Thesis, *Department of Civil Engineering, Chalmers University of Technology*.

Murthy M.V.V.S., Gopalakrishnan S., Nair P.S. (2007): A New Locking Free Higher Order Finite Element Formulation for Composite Beams. *CMC: Computers, Materials & Continua,* Vol. 5, No. 1, pp. 43-62.

Ngo D., Scordelis A. C. (1967): Finite element analysis of Reinforced Concrete Beams. *ACI Journal*, vol. 64, no. 3, pp. 152-163.

Nilson A. H. (1972): Internal measurement of bond-slip. *ACI Journal*, vol. 69, no. 7, pp. 439-441.

Nayak G. C., Zienkiewicz O. C. (1972): Elasto-Plastic Stress Analysis. *International Journal of Numerical Methods in Engineering*, vol. 5, pp. 113-135.

Oliveira R.S., Ramalho M.A., Correa M.R.S. (2008): A layered finite element for reinforced concrete beams with bond-slip effects. *Cement & Concrete composites* ,vol. 30, no. 10, pp. 245-252.

Rabczuk T., Akkermann J., Eibl J. (2005): A numerical model for reinforced concrete structures. *International Journal of solids and Structures*, vol. 42, pp. 1327-1354.

Samanta A. K., Ghosh S. (2008a): A 3D Computational Model of RC Beam Using Lower Order Elements with Enhanced Strain Approach in the Elastic Range. *Computers, Materials & Continua*, vol. 8, no. 1, pp. 43-52.

Samanta A. K., Ghosh S. (2008b): On Performance of EAS based Lower Order

Element in 3D Computational Modeling of RC Beam in the Elastic Range. *Proceedings of International Conference on Advances in Concrete and Construction (ICACC-2008), Hyderabad, India*, Feb 7-9, pp. 1084-1093.

Samanta A. K., Ghosh S. (2009): A 3D Hypoelastic Computational Model of Reinforced Concrete Structure. *Icfai Journal of Structural Engineering*, vol. II, no. 1, pp. 32-53.

Simo J. C., Rifai M. S. (1990): A class of mixed assumed strain methods and the method of incompatible modes. *International Journal for Numerical Methods in Engineering*, vol. 529, pp. 1595-1638.

Simo J. C., Armero F. (1992): Geometrically non-linear enhanced strain mixed methods and the method of incompatible modes. *Intl. Journal for Numerical Methods in Engineering*, vol. 33, pp. 1413-1449.

Souza Neto de E. A., Peric D. Dutko M., Owen D. R. J. (1990): Design of simple low order finite elements for large strain analysis of nearly incompressible solids. *International Journal of solids and structures,* vol. 33, pp. 3277-3296.

Sousa de R. J. A., Natal Jorge R. M., Valente A. F. Robert, Cesar de sa J. M. A., Arieas M. A. Pedro and Fernandes A. (2002): A. Lower order elements for 3D analysis. *5th world congress on Computational Mechanics(WCCM), Viena, Austria* July 7-12.

Sousa de R. J. A., Natal Jorge R. M., Valente A. F. Robert and Cesar de sa J. M. A. (2003a): A new volumetric and shear locking-free 3D enhanced strain element. *Engineering computations*, vol. 20, no. 7, pp. 896-925.

Sousa de R. J. A., Natal Jorge R. M., Valente A. F. Robert and Cesar de sa J. M. A. (2003b): Formulation of EAS solid elements for incompressibility and thin shell application in Nonlinear range. *VII International Conference on Computational Plasticity COMPLAS 2003*, Barcelona.

Valente A. F. Robert, Natal Jorge R. M., Cesar de sa J. M. A., Arieas M. A. Pedro. (2002): Application of the enhanced assumed strain concept towards the development of shear locking-free shell elements. *5th World Cong. on Computational Mech.(WCCM) Viena Austria* July 7-12, pp. 1-20.